

# Supernova matter at subnuclear densities as a resonant Fermi gas: Enhancement of neutrino rates

A. Bartl,<sup>1,2</sup> C. J. Pethick,<sup>3,4</sup> and A. Schwenk<sup>2,1</sup>

<sup>1</sup>*Institut für Kernphysik, Technische Universität Darmstadt, D-64289 Darmstadt, Germany*

<sup>2</sup>*ExtreMe Matter Institute EMMI, GSI Helmholtzzentrum für Schwerionenforschung GmbH, D-64291 Darmstadt, Germany*

<sup>3</sup>*The Niels Bohr International Academy, The Niels Bohr Institute,  
University of Copenhagen, Blegdamsvej 17, DK-2100 Copenhagen Ø, Denmark*

<sup>4</sup>*NORDITA, KTH Royal Institute of Technology and Stockholm University,  
Roslagstullsbacken 23, SE-10691 Stockholm, Sweden*

At low energies nucleon-nucleon interactions are resonant and therefore supernova matter at subnuclear densities has many similarities to atomic gases with interactions dominated by a Feshbach resonance. We calculate the rates of neutrino processes involving nucleon-nucleon collisions and show that these are enhanced in mixtures of neutrons and protons at subnuclear densities due to the large scattering lengths. As a result, the rate for neutrino pair bremsstrahlung and absorption is significantly larger below  $10^{13} \text{ g cm}^{-3}$  compared to rates used in supernova simulations.

PACS numbers: 97.60.Bw, 26.50.+x, 95.30.Cq, 26.60.+c

*Introduction.*— In the standard model of core-collapse supernovae, energy is transferred to outer parts of the star by neutrinos diffusing out from the stellar core, thereby expelling matter. Matter in the density range  $\rho \sim 10^{11} - 10^{13} \text{ g cm}^{-3}$  plays an important role after core bounce, because under these conditions neutrinos decouple from the matter [1]. In this Letter, we calculate rates of neutrino processes in this regime. We find that nucleon-nucleon (NN) interactions, which are resonant at low energies (as is reflected in the weak binding of the deuteron) significantly enhance neutrino rates.

In neutral-current neutrino-nucleon processes, the axial vector part of weak interactions dominates. For a system consisting of neutrons alone, only noncentral parts of NN interactions contribute, whereas when both neutrons and protons are present, the central part also enters because the axial charges of the neutron and proton are unequal. In numerical simulations of stellar collapse, rates of neutrino processes are commonly treated in the one-pion-exchange approximation for NN interactions [2] and rates for matter containing both neutrons and protons are then obtained by replacing the neutron density by the total nucleon density. Neutrino processes in degenerate neutron matter have been studied based on more realistic NN scattering amplitudes by Hanhart *et al.* [3], who used free-space scattering amplitudes expressed in terms of experimentally determined phase shifts, and by Bacca *et al.* [4, 5], who also considered nondegenerate conditions and chiral effective field theory (EFT) interactions. Effects of neutron-proton collisions have been discussed in a number of works, including that of Friman and Maxwell [6] for degenerate matter in the context of neutron star cooling, and that of Sigl [7] directed towards processes in supernovae.

In this Letter, we investigate the rate of neutrino processes in matter at subnuclear densities taking into account the resonant nature of NN interactions. The basic

input for calculations of rates of neutrino processes is the axial charge-density structure factor [8]

$$S_A(\mathbf{q}, \omega) = \frac{\sum_{m,n} e^{-E_m/T} |\langle m | \rho_A(\mathbf{q}) | n \rangle|^2 \delta(\omega - E_n + E_m)}{\sum_m e^{-E_m/T}}, \quad (1)$$

where  $\mathbf{q}$  and  $\omega$  are the momentum and energy transfers, the states  $|m\rangle$  and  $|n\rangle$  are eigenstates of the nucleonic system,  $\rho_A(\mathbf{q})$  is the Fourier transform of the axial charge-density operator, and  $T$  is the temperature.  $S_A$  is related to the axial charge-density correlation function  $\chi_A$  by

$$S_A(\mathbf{q}, \omega) = \frac{1}{\pi n} \frac{1}{1 - e^{-\omega/T}} \text{Im} \chi_A(\mathbf{q}, \omega), \quad (2)$$

where  $n$  is the total density of nucleons. (We work in units where  $\hbar$ ,  $c$  and the Boltzmann constant are unity.) From  $S_A(\mathbf{q}, \omega)$  one can calculate the rates of neutrino scattering and of neutrino pair creation and annihilation.

In most calculations, the approach adopted is to use the nonrelativistic limit for the coupling of the axial field to the nucleons, in which case its strength is given by the spin operator times the axial charge of the nucleon  $C_A$ . For small momentum and energy transfers, the axial charge may be taken to be a constant, but more generally there are momentum-dependent and two-body current contributions [9]. Below we shall discuss the values for the axial charges. Strong interactions are included at different levels in the structure factor: at low densities directly from two-body scattering data, and in general based on NN interactions. One technical point is that the scattering amplitudes required to calculate the structure factor are generally off-shell ones, and therefore it is necessary to specify the energy at which the scattering amplitude is evaluated. This is particularly important at low energies because the interactions are resonant. The aim of the present work is to give a first estimate of the

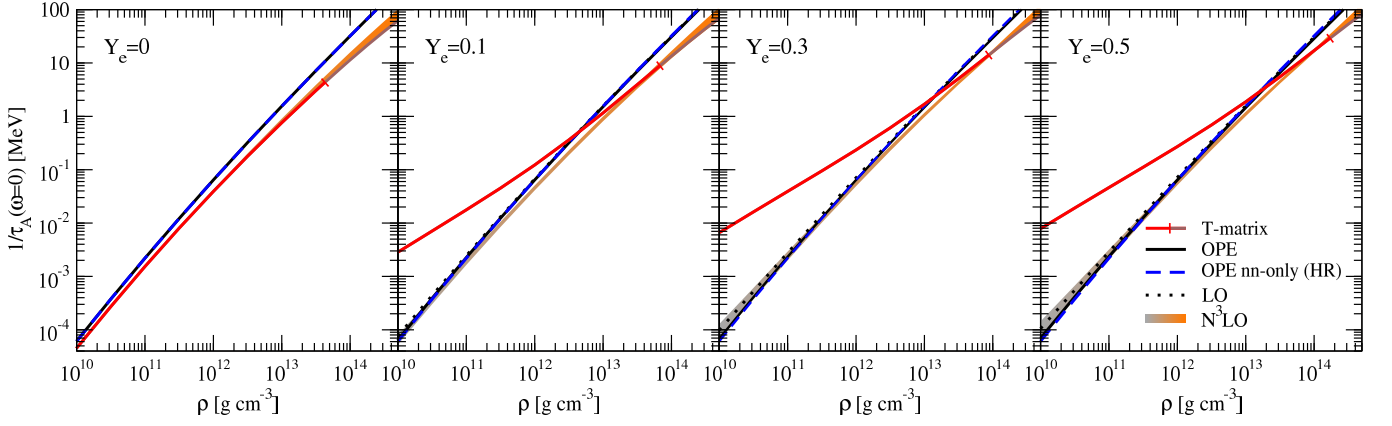


FIG. 1. (Color online) Spin relaxation rate  $1/\tau_A$  for  $\omega = 0$  as a function of density  $\rho$  for different electron fractions  $Y_e$  (from neutron matter to symmetric nuclear matter). The temperature is taken along typical supernova conditions, Eq. (11). Results are shown for the one-pion-exchange (OPE) approximation, the approximation used in supernova simulations (OPE nn-only, HR) [2], leading-order (LO) chiral EFT interactions, and including NN interactions at  $N^3\text{LO}$  at the Born level (for details see text). In addition, we show the results based on NN phase shifts ( $T$ -matrix). The color change from grey to orange indicates that the  $N^3\text{LO}$  results should only be trusted at higher densities where the Born approximation works well. The  $T$ -matrix results are expected to be valid up to a fugacity of  $z = 1/2$ , which is marked by the small bar.

effects of NN scattering, and therefore we shall, as a first approximation, evaluate scattering amplitudes for an energy equal to the mean of the energies of the initial and final states. A deeper investigation of this problem is left for future work. There are also contributions from three- and higher-body interactions, but at subnuclear densities, which appear to be particularly important in core-collapse supernovae, these are expected to be small.

*Axial response function.*— The basic picture that we shall adopt is to consider the nuclear medium as a system of interacting quasiparticles [4, 5, 10, 11]. To make the treatment more transparent, we do not include mean-field effects, because at subnuclear densities they are expected to be relatively unimportant for neutral currents. For zero frequency  $\chi_A$  at long wavelengths is given by [12]

$$\chi_A^0 = \sum_{i=np} \sum_1 (C_A^i \sigma_1)^2 \left( -\frac{\partial n_1^i}{\partial \epsilon_1^i} \right). \quad (3)$$

Here we use the shorthand notation  $1 \equiv (\mathbf{p}_1, \sigma_1)$  for momentum and spin.  $n_1^i$  is the quasiparticle distribution function for species  $i = n, p$ , and  $\epsilon_1^i$  is the quasiparticle energy. Our approach to determine the frequency dependence follows Refs. [2, 7, 8] by calculating the response at frequencies high compared with a typical collision frequency, and then interpolating between the low- and high-frequency results by a single relaxation time  $\tau_A$ .

To calculate  $\chi_A$  at frequencies high compared with typical collision rates for nucleons, we generalize the formalism of Ref. [5] to mixtures of neutrons and protons. The only difference compared with the result for pure neutrons is that the particles can be either neutrons or protons. For  $q = 0$ , we find

$$\chi_A \approx \frac{i}{\omega} \frac{\chi_A^0}{\tau_A} \equiv \frac{i}{\omega} \Upsilon_A \quad \text{with} \quad \Upsilon_A = \Upsilon_A^{nn} + \Upsilon_A^{pp} + 2\Upsilon_A^{np}, \quad (4)$$

where the superscripts indicate the nucleons involved in the process. Finally, the expression for  $\chi_A$  that interpolates between the low- and high-frequency limits is

$$\chi_A = \frac{\chi_A^0}{1 - i\omega\tau_A}. \quad (5)$$

As a preview of our results for the spin relaxation rate in mixtures of neutrons and protons, we refer to Fig. 1.

The different NN contributions  $\Upsilon_A^{ij}$  are given by

$$\begin{aligned} \Upsilon_A^{ij} &= \frac{1}{1 + \delta_{ij}} \frac{2\pi}{4\omega} \sum_{1234} \delta_\epsilon^+ \delta_{\mathbf{p}} \left| \langle 34 | \mathcal{T}^{ij} | 12 \rangle \right|^2 \\ &\times \left[ n_1^i n_2^j (1 - n_3^i)(1 - n_4^j) - n_3^i n_4^j (1 - n_1^i)(1 - n_2^j) \right] \\ &\times (C_A^i \sigma_1 + C_A^j \sigma_2 - C_A^i \sigma_3 - C_A^j \sigma_4)^2, \end{aligned} \quad (6)$$

which is an even function of  $\omega$ . Here,  $\delta_\epsilon^+ \equiv \delta(\omega + \epsilon_1^i + \epsilon_2^j - \epsilon_3^i - \epsilon_4^j)$  and  $\delta_{\mathbf{p}} \equiv \delta(\mathbf{p}_1 + \mathbf{p}_2 - \mathbf{p}_3 - \mathbf{p}_4)$  are energy and momentum conserving delta functions. We will employ scattering amplitudes  $\mathcal{T}^{ij}$  that include exchange contributions, and the factor of  $1/(1 + \delta_{ij})$  in Eq. (6) is to avoid double-counting of final states for collisions between particles of the same species. Thus

$$\begin{aligned} \Upsilon_A^{ij} &= \frac{\pi}{\omega} \sum_{1234} \delta_\epsilon^+ \delta_{\mathbf{p}} \left| \langle 34 | \mathcal{T}^{ij} | 12 \rangle \right|^2 \\ &\times \left[ n_1^i n_2^j (1 - n_3^i)(1 - n_4^j) - n_3^i n_4^j (1 - n_1^i)(1 - n_2^j) \right] \\ &\times \begin{cases} C_A^{i2} \sigma_1 (\sigma_1 + \sigma_2 - \sigma_3 - \sigma_4) & \text{for } i = j, \\ C_A^{i2} \sigma_1 (\sigma_1 - \sigma_3) + C_A^{j2} \sigma_2 (\sigma_2 - \sigma_4) \\ + 2C_A^i C_A^j \sigma_1 (\sigma_2 - \sigma_4) & \text{for } i \neq j. \end{cases} \end{aligned} \quad (7)$$

To separate the spin sums from the phase space inte-

gration in  $\Upsilon_A^{ij}$ , we introduce the quantities

$$W^{ij} = \frac{1}{12} \sum_{\sigma_i} \left[ \langle 34 | \mathcal{T}^{ij} | 12 \rangle^* \sigma_1 \right. \\ \left. \times \begin{cases} C_A^{i2} [\sigma_1 + \sigma_2, \langle 34 | \mathcal{T}^{ij} | 12 \rangle] & \text{for } i = j, \\ (C_A^{i2} + C_A^{j2}) [\sigma_1, \langle 34 | \mathcal{T}^{ij} | 12 \rangle] \\ + 2 C_A^i C_A^j [\sigma_2, \langle 34 | \mathcal{T}^{ij} | 12 \rangle] & \text{for } i \neq j. \end{cases} \right] \quad (8)$$

The  $W^{ij}$  depend only on  $P, p, p'$  and three angles specifying the orientation of the total momentum  $\mathbf{P} = \mathbf{p}_1 + \mathbf{p}_2 = \mathbf{p}_3 + \mathbf{p}_4$  and the relative momenta  $\mathbf{p} = (\mathbf{p}_1 - \mathbf{p}_2)/2$  and  $\mathbf{p}' = (\mathbf{p}_3 - \mathbf{p}_4)/2$ . As for pure neutrons [5], we can write the expressions for  $\Upsilon_A^{ij}$  in alternative forms by using  $n_\lambda^i/(1 - n_\lambda^i) = e^{-(\epsilon_\lambda^i - \mu^i)/T}$  and the invariance of interactions under time reversal. We shall assume that the quasiparticle energy is of the form  $\epsilon_{\mathbf{p}}^i = \epsilon_0^i + p^2/(2m_i^*)$ ,

where  $m_i^*$  is the effective mass.

In the nondegenerate limit,  $\chi_A^0 = \sum_{i=np} C_A^{i2} n_i/T$ , and if  $\Upsilon^{ij}$  is independent of  $\mathbf{P}$ , we can finally write

$$\Upsilon_A^{ij} = \frac{n_i n_j \sinh(\omega/2T)}{\omega \pi \sqrt{2\pi m_{ij}^* T^3}} e^{-\omega/2T} \int_0^\infty dp p^2 e^{-p^2/(2m_{ij}^* T)} \\ \times \int_{-1}^1 d \cos \theta \sqrt{p^2 + 2m_{ij}^* \omega} W^{ij}, \quad (9)$$

where  $m_{ij}^*$  is the reduced mass for quasiparticles of species  $i$  and  $j$ , and  $\cos \theta = \hat{\mathbf{P}} \cdot \hat{\mathbf{p}}$ . For definiteness, we have taken  $\omega$  to be positive. For negative  $\omega$ , the lower limit of the  $p$  integral is determined by the condition that the square root vanishes. The integral is symmetrical in  $p$  and  $p'$  since  $2dp p^2 \sqrt{p^2 + 2m_{ij}^* \omega} = pp' dp^2 = pp' dp'^2$ .

In addition, we can expand  $\Upsilon_A^{ij}$  in partial waves:

$$\Upsilon_A^{ij} = 16\sqrt{\pi} n_i n_j \frac{\sinh(\omega/2T)}{\omega \sqrt{2m_{ij}^* T^3}} \int_0^\infty dp p^2 \sqrt{p^2 + 2m_{ij}^* \omega} e^{-p^2/(2m_{ij}^* T) - \omega/(2T)} \sum_{S\bar{S}T\bar{T}} \sum_{Ll'J\bar{J}} (-1)^{L+J+\bar{J}} \left( \hat{L} \hat{J} \hat{J} \right)^2 \frac{\hat{l}'}{\hat{S} \hat{S}} \\ \times \left( 1 - (-1)^{l+S+T} \right) \left( 1 - (-1)^{l+\bar{S}+\bar{T}} \right) \begin{Bmatrix} l' & l & L \\ l & l' & 0 \end{Bmatrix} \begin{Bmatrix} l' & l & L \\ S & S & J \end{Bmatrix} \begin{Bmatrix} l & l' & L \\ \bar{S} & \bar{S} & \bar{J} \end{Bmatrix} \langle p | \mathcal{T}_{\nu I J S}^{ij, T} | p' \rangle \langle p' | \mathcal{T}_{\nu' \bar{J} \bar{S}}^{ij, \bar{T}} | p \rangle \\ \times \sum_{M_S M'_S} C_{L\Delta M_S S M'_S}^{S M_S} C_{L\Delta M_S \bar{S} M'_S}^{\bar{S} M_S} \begin{cases} C_A^{i2} M_S \Delta M_S & \text{for } i = j, \\ \frac{1}{8} (C_A^{i2} + C_A^{j2}) (1 - M_S M'_S) + \frac{1}{2} C_A^i C_A^j (M_S \Delta M_S - \frac{1}{2} (1 - M_S M'_S)) & \text{for } i \neq j. \end{cases} \quad (10)$$

where  $\hat{a} \equiv \sqrt{2a+1}$  and  $\Delta M_S \equiv M_S - M'_S$ , and the sums for  $i = j$  collapse to  $S = \bar{S} = T = \bar{T} = 1$ .

*Results.* – Because we focus on relatively low densities, we neglect effective mass effects and use  $m_n^* = m_n^* = 939$  MeV. For the axial charges, we take  $C_A^p = -C_A^n = g_A/2 = 1.26/2$  and note that strange quark contributions, as discussed in Ref. [13], are rather uncertain and do not change our results significantly. We consider different electron fractions  $Y_e$  from pure neutron to symmetric matter and take for the temperature  $T$  typical values in supernovae [5],

$$T = 3 \text{ MeV} \left( \frac{\rho}{10^{11} \text{ g cm}^{-3}} \right)^{1/3}, \quad (11)$$

which corresponds to nondegenerate matter, except for  $\rho > 10^{14} \text{ g cm}^{-3}$  where neutrino processes are ineffective.

Figure 1 shows the spin relaxation rate  $1/\tau_A$  for  $\omega = 0$  as a function of  $\rho$  for different  $Y_e$ . First, we consider the one-pion-exchange (OPE) approximation [14], as well as the typical approximation used in supernova simulations (OPE nn-only, HR), which uses the neutron-neutron

OPE rates of Hannestad and Raffelt [2] also for neutron-proton mixtures by replacing the neutron density by the total nucleon density. Note that we only apply this prescription for the results labeled HR. Figure 1 shows that the results at the OPE level are largely insensitive to the proton fraction and to this approximation.

A qualitatively similar dependence is found including all NN interactions at N<sup>3</sup>LO (also at the Born level), where the band in Fig. 1 is spanned by the EM 500 MeV, EGM 450/500 MeV and EGM 450/700 MeV potentials [16, 17]. These chiral EFT interactions were recently found to be perturbative at nuclear densities in neutron matter [18]. At the N<sup>3</sup>LO level, we find a very weak dependence on  $Y_e$  as well. As in the case of pure neutron matter [5], the N<sup>3</sup>LO rates are typically a factor of two smaller at higher densities than the OPE approximation, while they are similar at lower densities.

At low densities, the typical momenta are also low, so that the leading-order (LO) chiral EFT interactions are reliable. These include, in addition to OPE, two central contact interactions  $V_{\text{ct}}^{\text{LO}} = C_S + C_T \sigma_1 \cdot \sigma_2$ . For neutrons only,  $V_{\text{ct}}^{\text{LO}}$  does not contribute because it commutes with

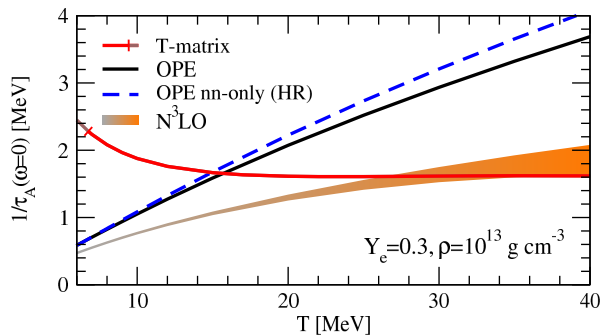


FIG. 2. (Color online) Spin relaxation rate  $1/\tau_A(\omega = 0)$  as a function of temperature  $T$  for  $Y_e = 0.3$  and  $\rho = 10^{13} \text{ g cm}^{-3}$ . Results are shown for the different cases as in Fig. 1.

the total spin  $\sigma_1 + \sigma_2$  in  $W^{ii}$ . Also the  $C_S$  part commutes with the spin operators in  $W^{ij}$ . However, due to the different axial charges for neutrons and protons, the spin-spin part  $C_T$  contributes in mixtures. This leads to an increase at low densities compared to OPE, shown in Fig. 1 by the dotted line (LO) for the EM 500 MeV value of  $C_T$ . This increase is small due to the approximate Wigner symmetry with large scattering lengths in both S waves, implying a small  $C_T$  value.

At low energies, NN interactions are resonant, so it is necessary to go beyond the Born approximation. For low densities and nondegenerate conditions, the spin relaxation rate can be determined model independently from the  $T$ -matrix based on NN phase shifts, similar to the virial expansion for energy contributions [19]. The resulting  $1/\tau_A$  based on the Nijmegen partial wave analysis [20] is shown in Fig. 1. For neutron matter, they agree well with the  $N^3\text{LO}$  results [5], because central interactions do not contribute. In mixtures of neutrons and protons, we find a dramatic enhancement at subnuclear densities  $\rho \lesssim 10^{13} \text{ g cm}^{-3}$  compared to the OPE rates used in supernova simulations. This enhancement is due to the large scattering lengths (see Fig. 3). The  $T$ -matrix results are expected to be valid up to a fugacity of  $z \approx n_n \lambda_n^3 / 2 \lesssim 1/2$ , where  $\lambda_n$  is the thermal wavelength. This is indicated by the small bar in Fig. 1. Interestingly, around this point and for higher densities, the  $T$ -matrix and  $N^3\text{LO}$  results agree well. This is because NN interactions become weaker at higher energies.

In the nondegenerate limit, the energy scale of the collision is set by the temperature. Therefore, we find the same enhancement of the rate with decreasing temperature, as shown in Fig. 2. For higher temperatures, both  $T$ -matrix and  $N^3\text{LO}$  results are a factor of  $\sim 2$  smaller compared to the OPE approximation.

The enhancement of the rates can be traced to the large scattering lengths. To this end, we study in Fig. 3 various approximations for the  $T$ -matrix. At low densities,  $1/\tau_A$  is dominated by the S-wave contributions, mostly from the scattering lengths. If we only keep the scatter-

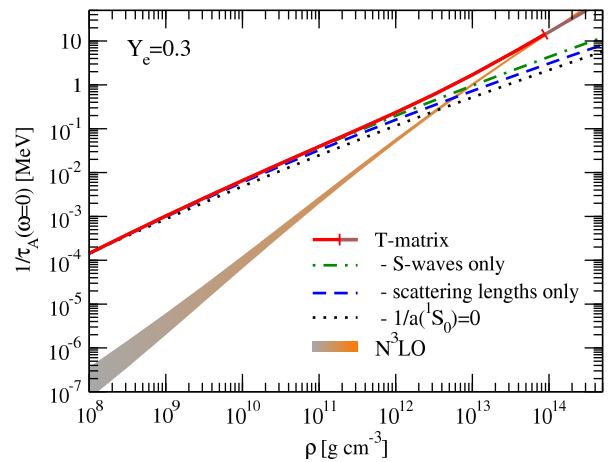


FIG. 3. (Color online)  $T$ -matrix results for  $1/\tau_A(\omega = 0)$  as a function of density  $\rho$  for  $Y_e = 0.3$ , with temperature along supernova conditions (11). The full  $T$ -matrix results (solid line) are compared to including only S-waves (dash-dotted line), only S-wave scattering lengths (dashed line), and finally also setting the  $^1S_0$  scattering length to infinity (dotted line). For comparison, the  $N^3\text{LO}$  results are also shown.

ing lengths and also take  $1/a(^1S_0) = 0$ , the low-density behavior can be reproduced with the simple expression characterized by the  $a(^3S_1)$  scattering length only

$$\frac{1}{\tau_A(\omega = 0)} \approx \frac{8\pi n_n n_p x}{n\sqrt{2\pi T}(m_{np}^*)^{3/2}} e^x \Gamma(0, x), \quad (12)$$

where  $1/x = 2m_{np}^* T (a(^3S_1))^2$  and  $\Gamma$  is the incomplete gamma function.

To explore the astrophysical impact of our findings, we show in Fig. 4 the energy-averaged inverse mean-free path of a neutrino against pair absorption (see Refs. [2, 11]). For the conditions (11), the inverse mean-free path is enhanced for densities  $\rho \lesssim 10^{12} \text{ g cm}^{-3}$ . For a fixed neutrino energy, the opacity enhancement increases with decreasing neutrino energy. Figure 4 shows again how close the  $T$ -matrix and  $N^3\text{LO}$  results are for higher densities. Combined with the reduction of the opacity at higher densities, this can contribute to energy transport from hotter matter at higher densities to regions further out (see the comparison in the bottom panel to the OPE approximation used in supernovae). This requires detailed simulations that include competing neutrino processes at these densities. Finally, the enhanced rates in mixtures also contribute to inelastic scattering from NN pairs, which is the analog of neutrino deuteron breakup when deuterons are dissolved [21].

In this Letter, we have studied neutrino processes involving NN collisions in supernova matter at subnuclear densities. Due to the resonant nature of NN interactions this regime has many similarities to atomic gases with interactions dominated by a Feshbach resonance. After generalizing the relaxation rate formalism to mixtures of

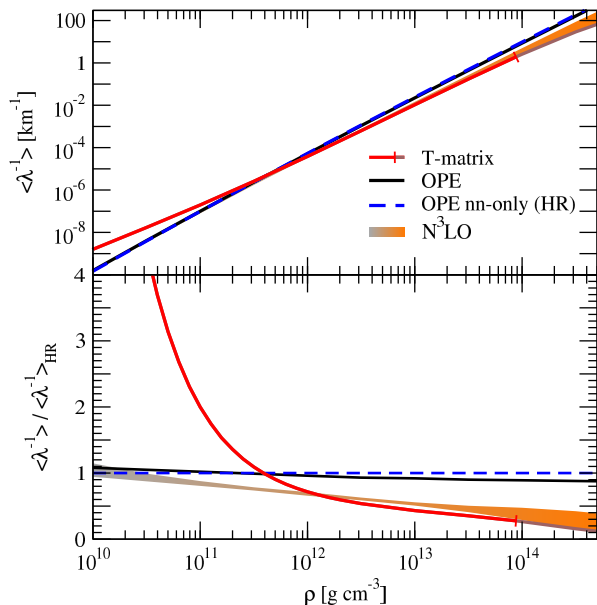


FIG. 4. (Color online) Top panel: Energy-averaged inverse mean-free path ( $\lambda^{-1}$ ) of a neutrino against pair absorption as a function of density  $\rho$  for  $Y_e = 0.3$ , with temperature along supernova conditions (11). We assume a Boltzmann distribution for the neutrino and antineutrino. Results are shown for the different cases as in Fig. 1. Bottom panel: Same, but normalized to the approximation used in supernova simulations (OPE nn-only, HR) [2].

neutrons and protons, we have shown that in mixtures the rates for neutrino pair bremsstrahlung and absorption are enhanced for  $\rho \lesssim 10^{13} \text{ g cm}^{-3}$  due to the large scattering lengths. Compared to rates used in supernova simulations, we find a reduction of the rates at higher densities. Combined with the enhancement at lower densities, this can provide an interesting mechanism for energy transport to the outer layers.

We thank S. Bacca, A. Gezerlis, and H.-Th. Janka for useful discussions. This work was supported by BMBF ARCHES, the ERC Grant No. 307986 STRONGINT, the Helmholtz Alliance HA216/EMMI, and the Studienstiftung des deutschen Volkes.

- [1] For a recent review, see, e.g., H.-T. Janka, *Annu. Rev. Nucl. Part. Sci.* **62**, 407 (2012).
- [2] S. Hannestad and G. G. Raffelt, *Astrophys. J.* **507**, 339 (1998).
- [3] C. Hanhart, D. R. Phillips, and S. Reddy, *Phys. Lett. B* **499**, 9 (2001).
- [4] S. Bacca, K. Hally, C. J. Pethick, and A. Schwenk, *Phys. Rev. C* **80**, 032802(R) (2009).
- [5] S. Bacca, K. Hally, M. Liebendörfer, A. Perego, C. J. Pethick, and A. Schwenk, *Astrophys. J.* **758**, 34 (2012).
- [6] B. Friman and O. Maxwell, *Astrophys. J.* **232**, 541 (1979).
- [7] G. Sigl, *Phys. Rev. D* **56**, 3179 (1997).
- [8] See, e.g., G. G. Raffelt, *Stars as Laboratories for Fundamental Physics* (University of Chicago Press, 1996).
- [9] See, e.g., J. Menéndez, D. Gazit, and A. Schwenk, *Phys. Rev. Lett.* **107**, 062501 (2011).
- [10] G. I. Lykasov, E. Olsson, and C. J. Pethick, *Phys. Rev. C* **72**, 025805 (2005).
- [11] G. I. Lykasov, C. J. Pethick, and A. Schwenk, *Phys. Rev. C* **78**, 045803 (2008).
- [12] A. Burrows and R. F. Sawyer, *Phys. Rev. C* **58**, 554 (1998).
- [13] G. G. Raffelt and D. Seckel, *Phys. Rev. D* **52**, 1780 (1995).
- [14] We have checked that the spin sums  $W^{ij}$  agree with previous results for neutron-proton bremsstrahlung of Refs. [6, 15] (note the typo in [6], see [15]).
- [15] D. Yakovlev, A. Kaminker, O. Y. Gnedin, and P. Haensel, *Phys. Rep.* **354**, 1 (2001).
- [16] D. R. Entem and R. Machleidt, *Phys. Rev. C* **68**, 041001 (2003).
- [17] E. Epelbaum, W. Glöckle, and U.-G. Meißner, *Nucl. Phys. A* **747**, 362 (2005).
- [18] T. Krüger, I. Tews, K. Hebeler, and A. Schwenk, *Phys. Rev. C* **88**, 025802 (2013).
- [19] C. J. Horowitz and A. Schwenk, *Nucl. Phys. A* **776**, 55 (2006).
- [20] V. G. J. Stoks, R. A. M. Klomp, M. C. M. Rentmeester, and J. J. de Swart, *Phys. Rev. C* **48**, 792 (1993); [www.nn-online.org](http://www.nn-online.org).
- [21] For a discussion of the impact of inelastic scattering from light nuclei, see, e.g., A. Arcones, G. Martínez-Pinedo, E. O'Connor, A. Schwenk, H.-Th. Janka, C. J. Horowitz, and K. Langanke, *Phys. Rev. C* **78**, 015806 (2008).